Materials Plus
https://ojs.wiserpub.com/index.php/mp/

Research Article

Advanced Frequency Study of Thick FGM Cylindrical Shells by Using TSDT and Nonlinear Shear

C.C. Hong

Department of Mechanical Engineering, Hsiuping University of Science and Technology, Taichung, 412406, Taiwan
E-mail: cchong@mail.hust.edu.tw

Received: 26 September 2023; **Revised:** 16 November 2023; **Accepted:** 29 November 2023

Abstract: For the advanced frequency study of thick functionally graded material (FGM) circular cylindrical shells, it is interesting to consider the extra effects of nonlinear coefficient term in third-order shear deformation theory (TSDT) of displacements on the calculation of varied shear correction coefficient. The formulation for the advanced nonlinear shear correction coefficient are based on the energy equivalence principle. The values of nonlinear shear correction coefficient are usually functions of nonlinear coefficient term of TSDT, power-law exponent parameter and environment temperature. The free vibration frequencies of thick FGM circular cylindrical shells are investigated with the simply homogeneous equation by considering that simultaneous effects of the TSDT, the nonlinear shear correction coefficient of transverse shear force and the two direction of mode shapes. The novelty is more important and reasonable for the thick FGM circular cylindrical shells, especially for the ratio of length to thickness is five by considering the effects of advanced nonlinear shear correction coefficient and nonlinear coefficient term of TSDT on the advanced calculation of fundamental first natural frequencies.

Keywords**:** advanced; nonlinear; shear correction; TSDT; FGM

1. Introduction

There are some traditional numerical investigations in the frequency study of free vibration for the functionally graded material (FGM) cylindrical shells and panels. Zhang et al. [1] presented the isogeometric numerical method and first-order shear deformation theory (FSDT) of displacements to study the natural frequencies and mode shapes for the carbon nanotubes reinforced (CNTR) FGM cylindrical shells. Liu et al. [2] presented the wave based method (WBM) and FSDT of displacements to study the natural frequency for the FGM cylindrical shells by considering the constant value of shear correction factor equal to 5/6 for the transverse shear force. Baghlani et al. [3] presented the Euler-Lagrange equations and higher-order shear deformation theory (HSDT) of displacements to study the natural frequency for the fluid-filled FGM cylindrical shells surrounded by Pasternak elastic foundation. Shahbaztabar et al. [4] presented the eigenvalue equation and FSDT of displacements to study the natural frequency for the fluid-filled FGM cylindrical shells surrounded by Pasternak elastic foundation by also considering the constant value of shear correction factor equal to 5/6 for the transverse shear force. Babaei et al. [5] presented the two steps perturbation technique and HSDT of displacements to study the natural frequency for the FGM cylindrical panels resting on nonlinear elastic foundation. Zhang et al. [6] presented the modified Fourier cosine series method and FSDT of displacements to study the natural frequency for the moderately thick FGM cylindrical shells by also considering the constant value of shear correction factor equal to 5/6 for the transverse shear force. Fan et al. [7] presented the Walsh series method (WSM) and FSDT of displacements to study the natural frequency for the FGM cylindrical shells by also considering the constant value

DOI: https://doi.org/10.37256/2220233711

of shear correction factor equal to 5/6 for the transverse shear force. Awrejcewicz et al. [8] presented the variational Ritz method, the R-functions method (RFM) and FSDT of displacements to study the natural frequency for the shallow FGM cylindrical shells by also considering the constant value of shear correction factor equal to 5/6 for the transverse shear force. Liew et al. [9] presented the eigenvalue equation and FSDT of displacements to study the natural frequency for the coating-FGM-substrate cylindrical shells by also considering the constant value of shear correction factor equal to 5/6 for the transverse shear force.

For the frequency study of free vibration in the thick FGM cylindrical shells, it is usually considered the shear correction factor effect in the transverse shear force. The author has some investigations in the computed and varied values for the shear correction factor. Hong [10] presented the preliminary studies in free vibration frequency of thick FGM circular cylindrical shells without considering the effects of nonlinear coefficient TSDT term on the varied shear correction coefficient calculation. Hong [11] presented the preliminary studies of the varied shear correction and FSDT effects on the vibration frequency of thick FGM circular cylindrical shells in unsteady supersonic flow. In the advanced study for the vibration frequency of thick FGM circular cylindrical shells with the simply homogeneous equation, it is interesting to consider the simultaneous effects of the TSDT of displacements, the nonlinear shear correction coefficient of transverse shear force and the two directions of mode shapes. The vibration frequency results vs. shear correction coefficient k_α values, nonlinear coefficient term c_1 of TSDT, FGM power-law exponent parameter and environment temperature are studied, respectively under four main cases of (a) advanced nonlinear k_α, c_1 = 0.333333/mm^2; (b) linear k_α, c_1 = 0/mm^2; (c) constant k_α = 5/6, c_1 = 0.333333/mm^2 and (d) constant k_α = 5/6, c_1 = 0/mm^2.

2. Formulation for the advanced nonlinear k_α

For a two-material thick FGM circular cylindrical shells problem model under environment temperature T with thickness h_1 of FGM constituent material 1 and thickness h_2 of FGM constituent material 2, respectively in the thickness direction of the cylindrical coordinate systems are shown in **Fig. 1**. The properties P_i of individual constituent material are in functions of T for the power-law function type of FGMs [12]. The time dependent of nonlinear displacements (u, v and w) at any point (x, θ, z) of thick FGM cylindrical shells are assumed in the nonlinear vs. z^3 with coefficient c_1 term of TSDT equations [13] as follows,

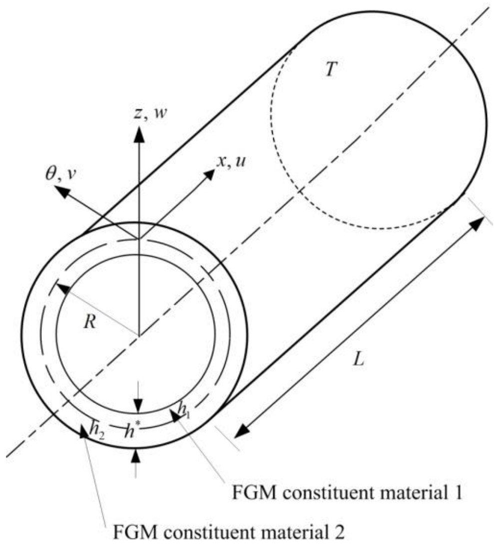

Figure 1. Two-material thick FGM circular cylindrical shells problem model

$$\begin{aligned} u &= u_0(x,\theta,t) + z\phi_x(x,\theta,t) - c_1 z^3\left(\phi_x + \frac{\partial w}{\partial x}\right), \\ v &= v_0(x,\theta,t) + z\phi_\theta(x,\theta,t) - c_1 z^3\left(\phi_\theta + \frac{\partial w}{R\partial \theta}\right), \\ w &= w(x,\theta,t), \end{aligned} \tag{1}$$

where u_0 and v_0 are the tangential displacements in the in-surface coordinates x and θ axes direction, respectively. w is the transverse displacement in the out of surface coordinates z axis direction of the middle-plane of shells. ϕ_x and ϕ_θ are the shear rotations. R is the middle-surface radius at any point (x , θ , z) of the FGM cylindrical shells. t is the time. The coefficient for $c_1 = 4/(3h^{*2})$ is given in the TSDT approach, in which h^* is the total thickness of FGM circular cylindrical shells.

For the normal stresses (σ_x and σ_θ) and the shear stresses ($\sigma_{x\theta}$, $\sigma_{\theta z}$ and σ_{xz}) in the thick FGM circular cylindrical shells under temperature difference ΔT for the (k)th constituent material are assumed in expressions of product matrix terms with stiffness $\bar{Q}_{ij}$, subscripts i,j=1,2,4,5,6, coefficients of thermal expansion $(\alpha_x, \alpha_\theta, \alpha_{x\theta})$ and strains $(\varepsilon_x, \varepsilon_\theta, \varepsilon_{x\theta}, \varepsilon_{\theta z}, \varepsilon_{x\theta})$ [10][14-15] as follows,

$$\begin{Bmatrix} \sigma_x \\ \sigma_\theta \\ \sigma_{x\theta} \\ \sigma_{\theta z} \\ \sigma_{xz} \end{Bmatrix}_{(k)} = \begin{bmatrix} \bar{Q}_{11} & \bar{Q}_{12} & \bar{Q}_{16} & 0 & 0 \\ \bar{Q}_{12} & \bar{Q}_{22} & \bar{Q}_{26} & 0 & 0 \\ \bar{Q}_{16} & \bar{Q}_{26} & \bar{Q}_{66} & 0 & 0 \\ 0 & 0 & 0 & \bar{Q}_{44} & \bar{Q}_{45} \\ 0 & 0 & 0 & \bar{Q}_{45} & \bar{Q}_{55} \end{bmatrix}_{(k)} \begin{Bmatrix} \varepsilon_x - \alpha_x \Delta T \\ \varepsilon_\theta - \alpha_\theta \Delta T \\ \varepsilon_{x\theta} - \alpha_{x\theta} \Delta T \\ \varepsilon_{\theta z} \\ \varepsilon_{xz} \end{Bmatrix}_{(k)} \tag{2a}$$

The stiffness integrations with z for the in-plane force resultant, moment and transverse shear force are expressed in the following equations,

$$(A_{i^s j^s}, B_{i^s j^s}, D_{i^s j^s}, E_{i^s j^s}, F_{i^s j^s}, H_{i^s j^s}) = \int_{\frac{-h^*}{2}}^{\frac{h^*}{2}} \overline{Q}_{i^s j^s} (1, z, z^2, z^3, z^4, z^6) dz \,, (i^s, j^s = 1,2,6)\,,$$
$$(A_{i^* j^*}, B_{i^* j^*}, D_{i^* j^*}, E_{i^* j^*}, F_{i^* j^*}, H_{i^* j^*}) = \int_{\frac{-h^*}{2}}^{\frac{h^*}{2}} k_\alpha \overline{Q}_{i^* j^*} (1, z, z^2, z^3, z^4, z^5) dz \,, (i^*, j^* = 4,5)\,, \tag{2b}$$

in which $\overline{Q}_{i^s j^s}$ $(i^s, j^s = 1,2,6)$ and $\overline{Q}_{i^* j^*}$ $(i^*, j^* = 4,5)$ are the stiffness of FGM shells. k_α is the advanced shear correction coefficient.

In the previous work of preliminary investigations for the computed and varied values of k_α are usually functions of total thickness of shells, FGM power law index and environment temperature [16]. For the advanced thick FGM cylindrical shells study, it is interesting to consider the extra effects of nonlinear coefficient term of TSDT displacements on the calculation of varied shear correction coefficient. The advanced shear correction factor k_α would be nonlinear with respect to c_1 can be obtained by using the energy equivalence principle. Let the total strain energy defined by the shear forces and transverse shears stresses, respectively in the form along the length of cylindrical shells by Whitney [15]. It is reasonable to assume that $\frac{\partial k_x}{\partial x} = \frac{\partial k_\theta}{\partial x} = \frac{\partial k_{x\theta}}{\partial x} = \frac{\partial k_x}{R\partial\theta} = \frac{\partial k_\theta}{R\partial\theta} = \frac{\partial k_{x\theta}}{R\partial\theta} = \frac{\partial nk_x}{\partial x} = \frac{\partial nk_\theta}{\partial x} = \frac{\partial nk_{x\theta}}{\partial x} = \frac{\partial nk_x}{R\partial\theta} = \frac{\partial nk_\theta}{R\partial\theta} = \frac{\partial nk_{x\theta}}{R\partial\theta}$, in which $k_x = \frac{\partial\phi_x}{\partial x}$, $k_\theta = \frac{1}{R}\frac{\partial\phi_\theta}{\partial\theta}$, $k_{x\theta} = \frac{\partial\phi_\theta}{\partial x} + \frac{1}{R}\frac{\partial\phi_x}{\partial\theta}$, $nk_x = \frac{\partial}{\partial x}(\phi_x + \frac{\partial w}{\partial x})$, $nk_\theta = \frac{1}{R}\frac{\partial}{\partial\theta}(\phi_\theta + \frac{\partial w}{R\partial\theta})$ and $nk_{x\theta} = \frac{\partial}{\partial x}(\phi_\theta + \frac{\partial w}{R\partial\theta}) + \frac{1}{R}\frac{\partial}{\partial\theta}(\phi_x + \frac{\partial w}{\partial x})$. With the same procedure as in the thick FGM plates by substituting the shear forces and transverse shear stresses equations, respectively into the total strain energy equation, thus the advanced k_α can be obtained as follows for the thick FGM circular cylindrical shells,

$$k_\alpha = \frac{1}{h^*}\frac{FGMZSV}{FGMZIV}\,, \tag{3}$$

where

$FGMZSV = (FGMZS - c_1 FGMZSN)^2$,

$FGMZIV = FGMZI - 2c_1 FGMZIV1 + {c_1}^2 FGMZIV2$, the expression of parameters *FGMZS*, *FGMZSN*, *FGMZ*I, *FGMZIV1* and *FGMZIV2* that are in functions of h^*, R_n, E_1 and E_2, for the more details can be referred by Hong [17]. The values of advanced nonlinear k_α are usually nonlinear in functions of c_1, R_n and T . In which R_n is the FGM power-law exponent parameter, E_1 and E_2 are the Young's modulus for the FGM constituent material 1 and constituent material 2, respectively. In the preliminary linear k_α study, it did not consider the effect of c_1 term in the calculation directly, thus the varied values of linear k_α are usually functions of h^*, R_n and T [16][18].

3. Some numerical results and discussions

The simply polynomial equation in fifth-order of λ_{mn} ($\lambda_{mn} = I_0\omega_{mn}{}^2$) [10] can be applied directly to calculate the free vibration ω_{mn} with considering the advanced nonlinear k_α, where subscript m is the axial half-waves number, n is the number of circumferential waves, and $I_i = \sum_{k=1}^{N^*}\int_k^{k+1}\rho^{(k)}z^i dz$, in which N^* is total number of constituent layers, $\rho^{(k)}$ is the density of (k)th constituent ply. The FGM temperature dependent constituent materials at inner material 1/outer material 2 i.e., SUS304/Si_3N_4 layers are used in the frequency computations of thick circular cylindrical shells. The advanced nonlinear values of k_α are usually functions of c_1, R_n and T. For geometric values of $L/R = 1$, $h_1 = h_2$ and $h^* = 1.2$ mm are used, in which L is the length of FGM cylindrical shells, the varied values of advanced nonlinear k_α are increasing with respect to R_n. Thus, advanced nonlinear values of k_α are used for frequency ω_{mn} computations of the free vibration including the coefficient c_1 term.

For the non-dimensional frequency parameter $f^* = 4\pi\omega_{11}R\sqrt{I_2/A_{11}}$ values under the effects of c_1 = 0.925925/mm^2 and c_1 = 0/mm^2 for L/h^*= 5, 8 and 10 are shown in **Table 1a**, where ω_{11} is the fundamental first natural frequency ($m = n = 1$). The presented f^* values under advanced k_α, environment temperature T and c_1 effects are not greater than 10.076400, which is in smaller value than 13.538765 in the preliminary k_α study case [10]. Another non-dimensional frequency parameter $\Omega = (\omega_{11}L^2/h^*)\sqrt{\rho_1/E_1}$ values under the cases of c_1 = 0.925925/mm^2 and c_1 = 0/mm^2 for L/h^*= 5, 8 and 10 are shown in **Table 1b**, in which ρ_1 is the density of FGM constituent material 1. The presented Ω values under advanced k_α, environment temperature T and c_1 effects are not greater than 26.945133, which is in smaller value than 32.380783 in the preliminary k_α study case [10]. The presented values of f^* vs. h^* under L/h^*=10, 300K, advanced nonlinear k_α and c_1 effects are shown in **Table 1c**. The presented value f^* = 8.429713 at c_1 = 0.333333/mm^2, h^* = 2mm, R_n = 0.5 is found. The presented values of Ω vs. h^* under L/h^*=10, 700K, advanced nonlinear k_α and c_1 effects are shown in **Table 1d**. The presented value Ω= 1.999438 at c_1 = 6.584362/mm^2, h^* = 0.45mm, R_n = 0.5 is found.

The natural frequency ω_{mn} (1/s) values with subscript mode shapes m and n are presented. The presented ω_{11} vs. R_n under $h^* = 1.2$ mm, advanced nonlinear k_α, environment temperature T and c_1 = 0.925925/mm^2 for L/h^*= 5 and 10 are shown in **Table 2**. There are in slightly different values for ω_{11} under L/h^*=5, R_n=0.5 and T=300K, e.g. ω_{11}=0.001911/s is in small different with ω_{11}=0.001906/s when compared with published paper [10]. The other presented ω_{mn} vs. m, n =2, 3, ...,9 are also found in the same value with published paper [10].

The advanced nonlinear k_α values for T =300K are listed in the **Table 3**. The values of advanced nonlinear k_α are independent of h^* for the thick FGM circular cylindrical shells. The values of k_α in the advanced nonlinear case with $c_1 \neq 0$ are different to the linear case with c_1 = 0. The different values of k_α vs. R_n under T =300K are shown in **Fig. 2**. There are in great variant k_α values under the advanced nonlinear case with $c_1 \neq 0$. The compared values of f^* vs. n at m= 1, 2 and 3 with L/h^*= 5, R_n = 0.5, h^* = 2mm, T =300K are shown in **Fig. 3**, respectively under four cases of (1) advanced nonlinear k_α, c_1 = 0.333333/mm^2; (2) linear k_α, c_1 = 0/mm^2; (3) constant k_α = 5/6, c_1 = 0.333333/mm^2 and (4) constant k_α = 5/6, c_1 = 0/mm^2. All of the presented frequencies f^* are decreasing vs. circumferential nodes *n*= 1-6 at axial nodes *m*= 1, 2 and 3 of thick FGM cylindrical shells. In **Fig. 3a**, f^* = 13.905487 is obtained at *m*= *n*= 1 under advanced nonlinear k_α, c_1 = 0.333333/mm^2. In **Fig. 3c**, f^* = 13.886978 is obtained at *m*= *n*= 1 under constant k_α = 5/6, c_1 = 0.333333/mm^2. In **Fig. 3b**, f^* = 20.434654 is obtained at *m*= *n*= 1 under linear k_α, c_1 = 0/mm^2. In **Fig. 3d**, f^* = 20.131851 is obtained at *m*= *n*= 1 under constant k_α = 5/6, c_1 = 0/mm^2. There are small effects of nonlinear coefficient term c_1 and k_α on the value of fundamental first natural frequencies by using the approaching of simply homogeneous equations. In the linear case c_1 = 0/mm^2, the values of f^* are overestimated. It is reasonable to consider the effect of nonlinear varied values k_α and c_1 on the advanced calculation of natural frequencies.

The article is presented for adding the effect of advanced nonlinear k_α as a continuation of a previous work [10] which was only using the effect of linear k_α. The advanced nonlinear k_α is expressed in eq. (3), in which the fraction parameters $FGMZSV$ and $FGMZIV$ are in nonlinear functions of c_1 value. For the linear k_α is preliminary expressed in eq. of the work [16], in which did not consider the effect of c_1 term in the calculation directly. The impact of the advanced nonlinear k_α on results are in clarification with previous work [10]. Comparing the fundamental value of f^* results in both articles they are calculated to differ by approximately 0.2%, when c_1 is not equal to zero, this corresponds to the nonlinear case. Notably, there is a discrepancy in results when c_1=0 (linear case), varying up to 40%. These compared values of f^* vs. *T* conclusion draws are shown in **Fig. 3e** for nonlinear k_α in this paper and linear k_α referred to [10].

For the more supplement of FGM and composited material analyses can be referred further in the fields of thermal analysis of cracked FGM plates by Do et al. [19], finite element method (FEM) applied in cracked nano-plates with flexo-electric effects by Doan et al. [20], and FEM used for triple-layer composite plates under moving load by Nguyen et al. [21].

Table 1a. f^* for SUS304/Si_3N_4

L/h^*	R_n	c_1 (1/mm^2)	f^*				
			Present solution, $h^* = 1.2$ mm, advanced k_α				
			T= 1K	*T*= 100K	*T*= 300K	*T*= 600K	*T*= 1000K
5	0.5	0.925925	3.180231	3.437422	3.883499	4.120175	3.663467
		0	5.373269	5.900316	6.836672	7.190872	5.986253
	1	0.925925	3.320887	3.575643	3.975845	0.922096	3.863254
		0	5.676170	6.208767	7.160784	7.515075	6.343256
	2	0.925925	3.492469	3.733553	4.141279	4.398373	4.100106
		0	5.922058	6.440915	7.375738	7.747935	6.706929
	10	0.925925	3.756472	3.984605	4.394351	4.670895	4.532107
		0	6.152549	6.615449	7.462710	7.898860	7.257466
8	0.5	0.925925	2.239428	2.420821	2.734613	2.901336	2.577111
		0	4.160760	4.516713	5.131114	5.437644	4.752500
	1	0.925925	2.337628	2.516835	10.076400	3.009658	2.716942
		0	4.345048	4.697000	5.307589	5.623309	5.000139
	2	0.925925	2.452844	3.294041	2.921348	3.102310	2.882582
		0	4.543049	4.886523	5.488020	5.817079	5.291233
	10	0.925925	2.643668	2.804904	3.095393	3.289649	3.186127
		0	4.871469	5.191528	5.766388	6.127082	5.840260
10	0.5	0.925925	1.926534	2.082611	2.352230	2.495704	2.217462
		0	3.864588	4.189507	4.749449	5.036603	4.427573
	1	0.925925	2.010933	2.165022	2.439111	2.586515	2.337732
		0	4.032133	4.352602	4.908469	5.204863	4.656122

2	0.925925	2.109406	5.662171	2.514311	2.670045	2.480144
	0	4.217228	4.530303	5.077848	5.386767	4.928913
10	0.925925	2.274468	2.413341	2.663402	2.830519	2.741575
	0	4.538136	4.830076	5.354484	5.691110	5.452303

Table 1b. Ω for SUS304/Si_3N_4

L/h^*	R_n	c_1 (1/mm²)	Ω				
			Present solution, $h^* = 1.2$ mm, advanced k_α				
			T= 1K	T= 100K	T= 300K	T= 600K	T= 1000K
5	0.5	0.925925	5.784212	6.106911	6.709765	7.146997	7.124487
		0	9.772912	10.482480	11.812148	12.473533	11.641697
	1	0.925925	5.787141	6.112288	6.644836	1.546665	7.126682
		0	9.891572	10.613412	11.967831	12.605302	11.701632
	2	0.925925	5.808020	6.121162	6.679326	7.116606	7.130050
		0	9.848456	10.559882	11.896074	12.536226	11.663293
	10	0.925925	5.784378	6.104845	6.696430	7.135295	7.126915
		0	9.473958	10.135582	11.372216	12.066360	11.412649
8	0.5	0.925925	6.516922	6.881316	7.559621	8.052412	8.018895
		0	12.108159	12.839003	14.184557	15.091719	14.787794
	1	0.925925	6.517866	6.883740	26.945133	8.077132	8.019266
		0	12.115031	12.846661	14.192934	15.091481	14.758296
	2	0.925925	6.526577	8.640930	7.538786	8.031305	8.020460
		0	12.088236	12.818329	14.162303	15.059334	14.722258
	10	0.925925	6.513334	6.875865	7.547174	8.040471	8.016496
		0	12.002076	12.726371	14.059581	14.975647	14.694459
10	0.5	0.925925	7.007969	7.399919	8.128190	8.658269	8.624771
		0	14.057844	14.886129	16.411842	17.473329	17.220947
	1	0.925925	7.008700	7.401881	8.152981	8.676906	8.624997
		0	14.053184	14.880881	16.407068	17.460603	17.178630
	2	0.925925	7.015937	18.566265	8.110490	8.640313	8.625900
		0	14.026609	14.854867	16.379774	17.431673	17.142679
	10	0.925925	7.004647	7.394999	8.117367	8.647848	8.622469
		0	13.976033	14.800395	16.319097	17.387567	17.147920

Table 1c. Frequency f^* with advanced nonlinear k_α

c_1 (1/mm²)	h^* (mm)	f^*		
		Present method, L/h^*=10, T= 300K, advanced nonlinear k_α ,		
		$R_n = 0.5$	$R_n = 1$	$R_n = 2$
6.584362	0.45	0.204179	0.215947	0.215343
0.925925	1.2	2.352230	2.439111	2.514311
0.333333	2	8.429713	8.724061	9.023207
0.000033	200	842669.2	871143.1	902712.1
0.000014	300	3801.353	3941.310	3940.774
0.000003	600	18914.72	19368.17	20173.66
0.000001	900	43945.85	45148.98	46948.40

Table 1d. Frequency Ω with advanced nonlinear k_α

c_1 (1/mm²)	h^* (mm)	Ω
		Present method, L/h^*=10, T= 700K, advanced nonlinear k_α

		$R_n = 0.5$	$R_n = 1$	$R_n = 2$
6.584362	0.45	1.999438	2.007078	1.966191
0.925925	1.2	8.663210	8.667815	8.642622
0.333333	2	18.63342	18.63708	18.61759
0.000033	200	18629.91	18630.04	18630.16
0.000014	300	55.19937	56.69650	59.67590
0.000003	600	140.1471	140.1418	139.0635
0.000001	900	217.3906	217.3800	216.3322

Table 2. Fundamental natural frequency ω_{11} for advanced nonlinear k_α, c_1, $h^* = 1.2$ mm

L/h^*	R_n	ω_{11} (1/s)				
		T= 1K	*T*= 100K	*T*= 300K	*T*= 600K	*T*= 1000K
5	0.5	0.001620	0.001731	0.001911	0.001951	0.001614
	1	0.001621	0.001733	0.001892	0.000422	0.001615
	2	0.001627	0.001735	0.001902	0.001943	0.001616
	10	0.001620	0.001731	0.001907	0.001948	0.001615
10	0.5	0.000490	0.000524	0.000578	0.000590	0.000488
	1	0.000491	0.000524	0.000580	0.000592	0.000488
	2	0.000491	0.001316	0.000577	0.000589	0.000488
	10	0.000490	0.000524	0.000578	0.000590	0.000488

Table 3. Advanced k_α vs. c_1 and R_n under *T*= 300K

c_1 (1/mm^2)	h^* (mm)	k_α						
		$R_n = 0.1$	$R_n = 0.2$	$R_n = 0.5$	$R_n = 1$	$R_n = 2$	$R_n = 5$	$R_n = 10$
92.592598	0.12	-0.821563	-0.861922	-1.181502	-4.392330	1.474843	0.583927	0.463616
0.925925	1.2	-0.821565	-0.861923	-1.181503	-4.392341	1.474844	0.583927	0.463617
0.231481	2.4	-0.821565	-0.861923	-1.181503	-4.392341	1.474844	0.583927	0.463617
0.037037	6	-0.821564	-0.861924	-1.181502	-4.392332	1.474843	0.583927	0.463617
0.009259	12	-0.821564	-0.861924	-1.181503	-4.392332	1.474843	0.583927	0.463617
0	0.12	0.898426	0.956500	1.087890	1.195721	1.226106	1.121959	1.019033
0	1.2	0.898426	0.956498	1.087891	1.195721	1.226106	1.121959	1.019034
0	2.4	0.898426	0.956498	1.087891	1.195721	1.226106	1.121959	1.019034
0	6	0.898425	0.956496	1.087891	1.195721	1.226106	1.121958	1.019033
0	12	0.898426	0.956495	1.087891	1.195721	1.226106	1.121958	1.019033

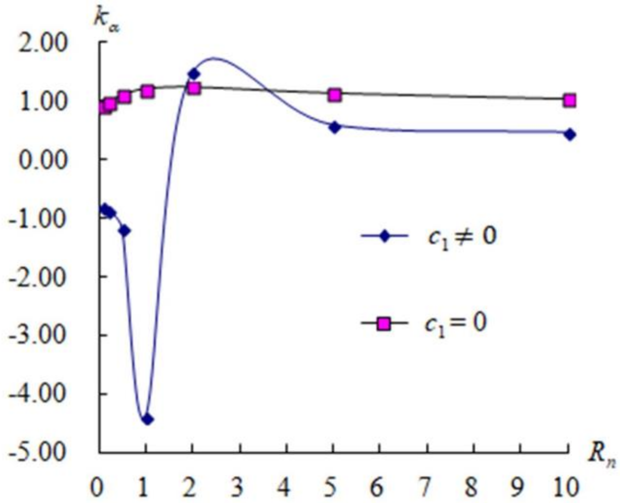

Figure 2. Values of k_α vs. R_n in nonlinear ($c_1 \neq 0$) and linear ($c_1 = 0$)

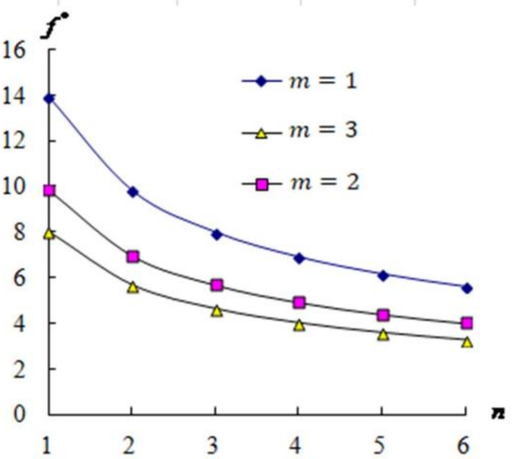

a

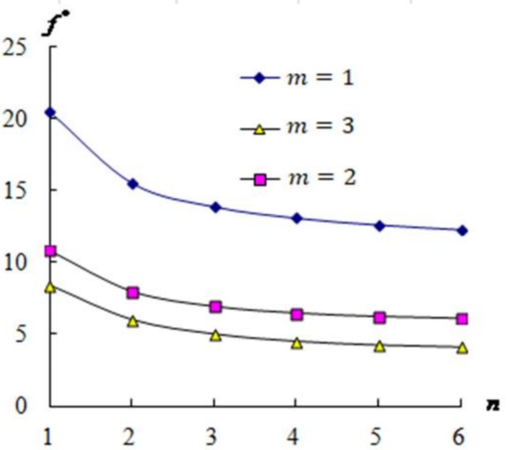

b

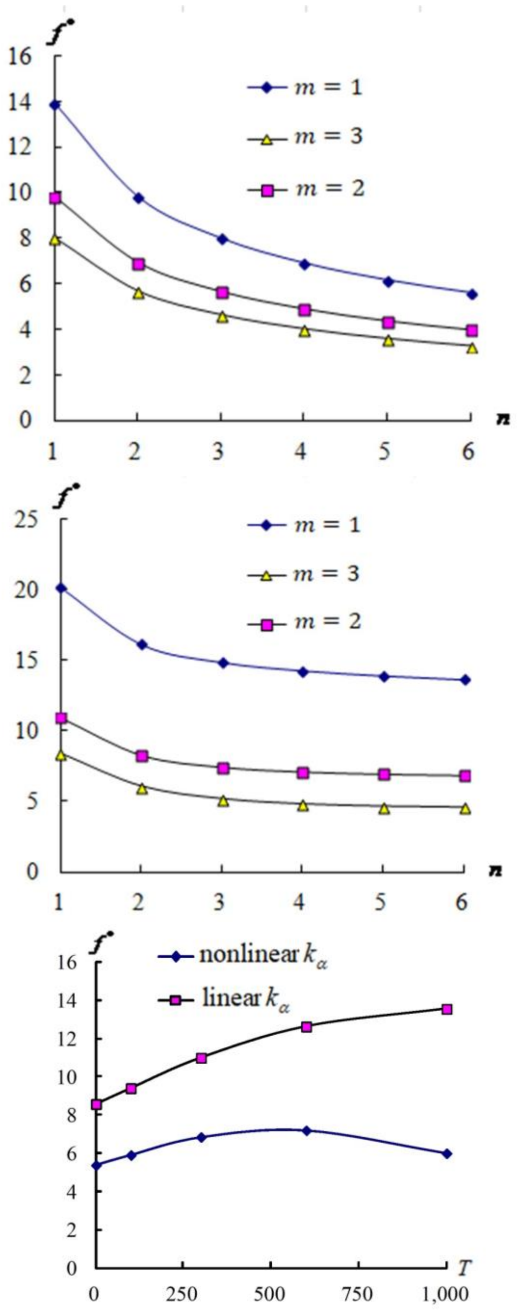

c

d

e

Figure 3. Compared f^* vs. *n* for *m*= 1-3, L/h^* = 5 with varied and constant k_α. **a** f^* vs. *n* for *m*= 1-3, L/h^* = 5 with advanced nonlinear k_α, c_1 = 0.333333/mm^2, **b** f^* vs. *n* for *m*= 1-3, L/h^* = 5 with linear k_α, c_1 = 0/mm^2, **c** f^* vs. *n* for *m*= 1-3, L/h^* = 5 with constant k_α = 5/6, c_1 = 0.333333/mm^2, **d** f^* vs. *n* for *m*= 1-3, L/h^* = 5 with constant k_α = 5/6, c_1 = 0/mm^2, **e** f^* vs. *T* for *m*=*n*=1, L/h^* = 5, h^* =1.2mm and c_1 = 0/mm^2

4. Conclusions

The advanced frequency values of free vibration are computed by using the simply homogeneous equation and advanced nonlinear k_α values for the thick FGM circular cylindrical shells. There are four parameters effects of nonlinear coefficient term c_1, shear correction coefficient k_α, power-law exponent parameter R_n and environment temperature T on the natural frequencies are investigated. The main results and new contributions of the research is more important and reasonable for the thick FGM circular cylindrical shells, especially for L/h^*=

5 to consider the effect of nonlinear varied values k_α and c_1 on the advanced calculation of fundamental first natural frequencies.

Acknowledgments

The author expresses his thanks to the people helping with this work, and acknowledge the valuable suggestions from the peer reviewers.

Conflict of interest

There is no conflict of interest for this study.

References

[1] Zhang, Y.; Jin, G.; Chen, M.; Ye, T.; Liu, Z. Isogeometric free vibration of sector cylindrical shells with carbon nanotubes reinforced and functionally graded materials. *Results Phys.* **2019**, *16*, 102889, https://doi.org/10.1016/j.rinp.2019.102889.

[2] Liu, T.; Wang, A.; Wang, Q.; Qin, B. Wave based method for free vibration characteristics of functionally graded cylindrical shells with arbitrary boundary conditions. *Thin-Walled Struct.* **2020**, *148*, https://doi.org/10.1016/j.tws.2019.106580.

[3] Baghlani, A.; Khayat, M.; Dehghan, S.M. Free vibration analysis of FGM cylindrical shells surrounded by Pasternak elastic foundation in thermal environment considering fluid-structure interaction. *Appl. Math. Model.* **2020**, *78*, 550–575. https://doi.org/10.1016/j.apm.2019.10.023.

[4] Shahbaztabar, A.; Izadi, A.; Sadeghian, M.; Kazemi, M. Free vibration analysis of FGM circular cylindrical shells resting on the Pasternak foundation and partially in contact with stationary fluid. *Appl. Acoust.* **2019**, *153*, 87–101, https://doi.org/10.1016/j.apacoust.2019.04.012.

[5] Babaei, H.; Kiani, Y.; Eslami, M.R. Large amplitude free vibrations of long FGM cylindrical panels on nonlinear elastic foundation based on physical neutral surface. *Compos. Struct.* **2019**, *220*, 888–898, https://doi.org/10.1016/j.compstruct.2019.03.064.

[6] Zhang, W.; Fang, Z.; Yang, X.-D.; Liang, F. A series solution for free vibration of moderately thick cylindrical shell with general boundary conditions. *Eng. Struct.* **2018**, *165*, 422–440, https://doi.org/10.1016/j.engstruct.2018.03.049.

[7] Fan, J.; Huang, J.; Zhang, J.; Zhang, J. The Walsh series method for free vibration analysis of functionally graded cylindrical shells. Composite Structures 2018, 206, 853–864.

[8] Awrejcewicz, J.; Kurpa, L.; Shmatko, T. Linear and nonlinear free vibration analysis of laminated functionally graded shallow shells with complex plan form and different boundary conditions. *Int. J. Non-linear Mech.* **2018**, *107*, 161–169, https://doi.org/10.1016/j.ijnonlinmec.2018.08.013.

[9] Liew, K.; Yang, J.; Wu, Y. Nonlinear vibration of a coating-FGM-substrate cylindrical panel subjected to a temperature gradient. *Comput. Methods Appl. Mech. Eng.* **2006**, *195*, 1007–1026, https://doi.org/10.1016/j.cma.2005.04.001.

[10] Hong, C.-C. Free Vibration Frequency of Thick FGM Circular Cylindrical Shells with Simply Homogeneous Equation by Using TSDT. *Adv. Technol. Innov.* **2020**, *5*, 84–97, https://doi.org/10.46604/aiti.2020.4380.

[11] Hong, C.C. Effects of Varied Shear Correction on the Thermal Vibration of Functionally-Graded Material Shells in an Unsteady Supersonic Flow. *Aerospace* **2017**, *4*, 12, https://doi.org/10.3390/aerospace4010012.

[12] Hong, C.C. Rapid Heating Induced Vibration of Magnetostrictive Functionally Graded Material Plates. *J. Vib. Acoust.* **2012**, *134*, 021019, https://doi.org/10.1115/1.4004663.

[13] Lee, S.; Reddy, J.; Rostam-Abadi, F. Transient analysis of laminated composite plates with embedded smart-material layers. *Finite Elements Anal. Des.* **2004**, *40*, 463–483, https://doi.org/10.1016/s0168-874x(03)00073-8.

[14] Lee, S.; Reddy, J. Non-linear response of laminated composite plates under thermomechanical loading. *Int. J. Non-linear Mech.* **2005**, *40*, 971–985, https://doi.org/10.1016/j.ijnonlinmec.2004.11.003.

[15] Whitney, J.M. *Structural Analysis Of Laminated Anisotropic Plates*; Taylor & Francis Ltd: London, United Kingdom, 2018; ISBN: 9780203738122.

[16] Hong, C. Thermal vibration of magnetostrictive functionally graded material shells by considering the varied effects of shear correction coefficient. *Int. J. Mech. Sci.* **2014**, *85*, 20–29, https://doi.org/10.1016/j.ijmecsci.2014.04.013.
[17] Hong, C.-C. Advanced Dynamic Thermal Vibration of Laminated FGM Plates with Simply Homogeneous Equation by Using TSDT and Nonlinear Varied Shear Coefficient. *Appl. Sci.* **2022**, *12*, 11776, https://doi.org/10.3390/app122211776.
[18] Hong, C.-C. Thermal Vibration of Thick FGM Circular Cylindrical Shells by Using TSDT. *Mater. Plus* **2022**, 2–11, https://doi.org/10.37256/mp.1120221967.
[19] Van Do, T.; Doan, D.H.; Tho, N.C.; Duc, N.D. Thermal Buckling Analysis of Cracked Functionally Graded Plates. *Int. J. Struct. Stab. Dyn.* **2022**, *22*, https://doi.org/10.1142/s0219455422500894.
[20] Doan, D.H.; Zenkour, A.M.; Van Thom, D. Finite element modeling of free vibration of cracked nanoplates with flexoelectric effects. *Eur. Phys. J. Plus* **2022**, *137*, 1–21, https://doi.org/10.1140/epjp/s13360-022-02631-9.
[21] Nguyen, H.N.; Nguyen, T.Y.; Tran, K.V.; Tran, T.T.; Nguyen, T.T.; Phan, V.D.; Do, T.V. A finite element model for dynamic analysis of triple-layer composite plates with layers connected by shear connectors subjected to moving load. Materials 2019, 12, 598.